TSGA10, a new player in regulating autophagy and apoptosis

Davood Rezazadeh (davoodrez@gmail.com)
Tehran University of Medical Sciences
Fatemeh Ranjbarnejad
Kermanshah University of Medical Sciences
Kamran Mansouri
Kermanshah University of Medical Sciences
Ali Mostafaie
Kermanshah University of Medical Sciences
Ebrahim Barzegari
Kermanshah University of Medical Sciences
Mohammad Hossein Modarressi
Tehran University of Medical Sciences

Research Article

Keywords: Apoptosis, Autophagy, BCL-2, TSGA10, Tumor suppressor

Posted Date: May 17th, 2022

DOI: https://doi.org/10.21203/rs.3.rs-1641538/v1

Abstract

Testis specific gene antigen 10 (TSGA10) overexpression could inhibit angiogenesis and tumor cell proliferation, migration and invasion through inhibiting HIF-1α. The exact role of TSGA10 in autophagy and apoptosis is not clear. Present study was conducted to investigate the potential effects of *TSGA10* overexpression on regulation of autophagy and apoptosis. To do so, TSGA10-containing vector (pcDNA3.1-TSGA10 vector) was designed for stable and transient transfections in HeLa cells, and clonal selection was applied. Expression of autophagy and apoptosis-related genes was assessed by real-time RT-PCR in TSGA10-overexpressing cells compared with HeLa cells transfected by empty vector. Rate of autophagy and cell viability were assessed by acridine orange and MTT assays, respectively. Our findings showed that overexpression of *TSGA10* would induce autophagy under normoxic and hypoxic conditions in the presence or absence of autophagy inducers. Expression levels of autophagy and apoptosis-related genes increased significantly in TSGA10-overexpressing cells compared with control cells. In addition, HeLa cells overexpressing *TSGA-10* exhibited lower expression of BCL-2 and survival rates in comparison with control cells. Molecular docking results showed that interaction between TSGA10 and BCL-2 could inhibit anti-apoptotic activity of BCL-2. According to our findings, *TSGA10* overexpression has a main role in regulating autophagy and apoptosis through inhibition of BCL-2. Therefore, *TSGA10* could be considered as a new regulator of autophagy and apoptosis in future studies.

Introduction

The testis specific gene antigen 10 (TSGA10) is an 82 kDa protein (accession number: AAH28366) expressed in dividing tissues such as testis, fetal differentiating tissues and various primary tumors. As illustrated by previous studies, TSGA10 plays an important role during the mitotic division, which is common to cancer, neurogenesis, embryogenesis and spermatogenesis. The full-length TSGA10 protein is post-translationally modified and finally cleaved in two parts; the first part, an N-terminal 27 kDa fragment is located in the Fibrous Sheath (FS) of sperm tail and the second one, a C-terminal 55 kDa fragment (1, 2). It has been reported that 55 kDa fragment of TSGA10 interacts with PASB domain of hypoxia-inducible factor-1α (HIF-1α) and prevents its dimerization leading to the inhibition of P300 recruitment, causes HIF-1α inactivation (2, 3). HIF-1α is a critical transcriptional regulator of the genes involved in many cellular processes. It has two major domains, named PASB (N-terminus) and TAD-C (C-terminus).

Due to important role of HIF-1α in various signaling pathways, the interaction between TSGA10 and HIF-1α results in dysregulated cell metabolism, cell growth, cell viability, angiogenesis, autophagy and apoptosis through modulated transcription of HIF-1α target genes (4). Autophagy is a normal process involving the sequestration of cytoplasmic parts and intracellular organelles in two layers membrane vacuole called the autophagosome. These vesicles merge with lysosomes and lead to degradation of the sequestered materials. This breakdown of cellular components supports cellular survival during starvation. Dysregulated autophagy is known to be involved in many human diseases and cancers (5). Recent investigations indicate that autophagy is a double-edged sword that may promote cancer cell

survival and growth in malignant neoplasms (6, 7). Furthermore, autophagy can induce cell death by a process termed autophagy-dependent cell death in certain cancer cell lines (8–10).

Autophagy and other programmed cell death such as apoptosis share molecular players and determine the overall fate of cell (11). Apoptosis is a type of cellular death initially characterized by its morphological characteristics, including cell shrinkage, chromatin condensation and nuclear cell fragmentation. Apoptosis is considered as a potential target in the cancer therapeutic approaches (12). Previous studies have demonstrated that TSGA10 is widely expressed in normal tissues and clearly is dysregulated in autoimmune diseases, solid tumors and leukemia. In some studies, it has been suggested as a cancer testis antigen (CTA) (13–15) and in other studies performed on tumor cells, it has been characterized as a tumor suppressor gene (3, 16). Because autophagy and apoptosis are considered as the main targets in many cancer treatments, in the present study, we investigated the potential effects of TSGA10 overexpression on autophagy and apoptosis in HeLa cells.

Materials And Methods

Chemicals and reagents

Primary Antibodies were goat anti-TSGA10, mouse anti-BCL-2, mouse anti-BAX, goat anti-Caspase-3, goat anti-LC3I and anti-LC3II (Santa Cruz, USA). Cisplatin, Ammonium chloride (NH4Cl) were purchased from Sigma. Rapamycin and G418 were purchased from Invivogen and Alexis Biochemicals, respectively. Acridine orange and Annexin V/PI kit were both obtained from Abcam and Sigma, respectively. Lipofectamine 2000, pcDNA3.1 and trypsin–EDTA were purchased from Invitrogen. T4 ligase was obtained from Takara Bio, Inc. All other reagents were obtained from Sigma-Aldrich (Taufkirchen, Germany).

Plasmid Constructions

The RT-PCR amplification mixture contained the following primers: 5'-AGGATCCGCCACCATGATGCGAAGTAGGTC-3' carrying a BamH1 site, underlined, and 5'-AGGAATTCGTCAGAAATCTCTGTAGC-3' carrying an EcoRI site, underlined, were designed for the TSGA10 gene's CDS (sequence coding for amino acids in protein, Accession NO. AF254756.1) domain. This sequence was amplified by RT-PCR with mentioned primers from 10 g human testis (3). The research protocol was approved by the research ethics committee on human experimentation of kermanshah university of medical sciences. Real-time RT-PCR conditions were as follows: denaturation at 94°C for 1 min, annealing at 60°C for 90 s, and extension at 72°C for 1 min for 35 cycles. Final extension was performed at 72°C for 10 min. The fragment carrying both the BamHI and EcoR1 site was acquired by RT-PCR. This RT-PCR protocol produced a 2115 bps fragment. The product was subjected to a double digestion with BamH1 and EcoR1 enzymes, and the digested DNA product was ligated into a 5.4 kb fragment of pcDNA3.1 (Invitrogen, USA) that was digested with the same enzymes. The ligated product was transformed into DH5α cells. Restriction endonuclease analysis, RT-PCR and plasmid sequencing were performed to validate the recombinant plasmid-reading frame.

Cell culture and transfection

HeLa cells (purchased from the Pasteur Institute of Iran) were considered as tumoral cells and human skin fibroblasts were isolated in a protocol described before, were considered as normal cells. STR profiling was performed to authenticate these cell lines (17). The cells were cultured in DMEM/F12 medium supplemented with 10% fetal bovine serum, 100 µg/mL streptomycin and 100 U/mL penicillin. Cells were maintained at 37°C in a humidified incubator with 5% CO2. Twelve hours before transfection, cells were seeded into a 24-well plate at a density of $1–2 \times 10^5$ cells per well. Cells were transfected when plate confluence was approximately 85–90%. For transient transfection, the cells were transfected with different vector concentrations (0.5 to 2 µg) using Lipofectamine 2000. For stable transfection, transfected HeLa cells were selected by culturting in medium containing 1 mg/ml of G418 for 4 weeks. Then positive cell clones were extracted and expanded into clonal cell strain. The HeLa cells transfected with TSGA10 containing plasmid or HeLa-pcDNA3.1-TSGA10 (H.pc-TSGA10) and empty plasmid-transfected cells HeLa-pcDNA3.1 (H.pc) were separately cultured in DMEM/F12. After obtaining stably transfected cells, the cells were continuously maintained in 200 µg/ml of G418. G418-resistant cells were analyzed for TSGA10 mRNA and protein expression by Real-time RT-PCR, western blot and immunocytochemistry analysis.

Cell viability assay

HeLa Cells were seeded at 5×10^3 cells per well in a 96-well plate and cultured with 10% fetal bovine serum (FBS) for 48 and 72 hours. The HeLa cell culture dishes were placed into a hypoxia chamber inside the cell culture incubator and exposed to hypoxia (1% oxygen). Hypoxia was obtained by flushing low oxygen gas (by injecting nitrogen to displace oxygen). Another set of cell culture dishes were cultured under normoxic condition. The cells were treated with 3- (4,5-dimethylthiazolyl-2)-2, 5-diphenyltetrazolium bromide (MTT, Sigma, USA) 20 µl/well [5 mg/ml in PBS] to measure cell viability. The purple-blue MTT formazan precipitate was dissolved in 200 µl of DMSO and swirled for 30 min. Absorbance was measured at 570 nm, with background subtraction of 630 using a spectrophotometer. This absorbance is also called optical density, which reflects the cell count and may be used to evaluate cell viability. Experiments were repeated six times.

Real-time RT-PCR

H.pc and H.pc-TSGA10 cell cultures were performed in hypoxic and normoxic conditions with or without 100 nM rapamycin as an autophagy inducer (18 h at 37°C, and 90% humidity). Total RNA were extracted from the cells using Trizol reagent (Invitrogen). Forward and reverse primers of target genes were designed by an acceptable primer design software. Real-time RT-PCR was performed using Takara Kit by Rotor Gene 6000 system (Corbett Research, Australia) in a 96-well plate (15 min at 95 °C, 40 cycles of 15 s at 95 °C, 15 s at 60 °C and 20 s at 72 °C). Finally, melting was done at 60–95°C (at an increment of 0.5°C per step and a holding time of 5 s for each step). Relative quantification analysis was performed using the Relative expression software tool (REST). The analysis used the sample's crossing point, the

efficiency of the reactions, the number of cycles completed and other values to compare the samples and create the ratios and results were reported as normalized ratios.

Western blot

HeLa Cells stably transfected with pcDNA3.1 and pcDNA3.1-TSGA10 plasmids cultured in normoxic and hypoxic conditions were analyzed by western blot. Protein lysates were incubated in 0.075 M Tris buffer (pH: 7.6) and 9 M Urea and were analyzed using the Bradford's method. Then 40-50 µg of total proteins underwent reducing SDS-PAGE using standard protocols. Then, sample proteins were transferred to a polyvinylidene fluoride membrane. The membrane was incubated with blocking buffer (PBS containing 5% non-fat milk) for 2 hours at 25 ˚C. The membranes were immunoblotted with respective primary antibodies and then incubated with specific secondary antibodies. After washing, TSGA10, BAX, BCL-2, Caspase-3, LC3I and LC3II were detected using a horseradish peroxidase-conjugated reaction. Protein levels were normalized relative to β-actin protein levels. The results were analyzed with TotalLab2 software (Wales, UK).

Acidic Vesicle Detection

Detection of acidic vesicle formation during autophagy was performed by acridine orange staining protocol followed by fluorescence analysis in normoxic and hypoxic conditions with and without rapamycin (Rap). In brief, H.pc and H.pc-TSGA10 cells were washed with PBS, fixed in 4% paraformaldehyde for 15 min at room temperature and then stained with acridine orange at 1 µg/µL final concentration for 30 min in the dark. Acridine orange can accumulate in acidic compartments, emitting bright red fluorescence detecting by fluorescence microscopy (Nikon, Japan, TS100). The intensity of this emission is proportional to the degree of acidity and volume of the compartment and demonstrated autophagy amount.

Molecular modeling and docking

Since there is no crystallographic coordinate file for TSGA10, homology modeling (HM) was used to model the structure. The sequence of TSGA10 (Q9BZW7) was obtained from Uniprot database. Suitable templates for HM (i.e. experimentally determined structures of high sequence identity with the TSGA10) were searched by querying Q9BZW7 against protein data bank on BLAST server (http://blast.ncbi.nlm.nih.gov/Blast.cgi), and 3S4R (vimentin central α-helical domain), 3CBU (putative glutathione S-transferase), 4IKM (CARD8), 1OBA (PHAGE CP-1), 4E61 (EB1-like motif of Bim1p) and 2IXU (Cpl-1 lysine) were chosen as the HM templates. HM using multiple templates can increase the accuracy and quality of the models developed, and is particularly suited for proteins with lower sequence identity (<40%) (18) which is the very situation.

Modeller-9.8 (19) was used to build homology models of TSGA10. From among the 1000 models generated, the one corresponding to the lowest value of the probability density function (pdf) and fewest restraints violations was selected for further analysis. An *ab initio* method implemented in the Modeller

which has been demonstrated to predict the conformations of loop regions, was used to refine some of the loops of the selected model. The overall stereochemical quality of the final developed 3D model for each TSGA10 was evaluated by the program PROCHECK (20).

The calculations regarding the interaction between TSGA10 and BCL-2 structures were carried out using HADDOCK web server (21), which makes use of chemical shift perturbation data to derive the docking while allowing various degrees of flexibility. The structure of BCL-2 was retrieved from the Protein Data Bank (1G5M). The docking procedure was performed in three steps as follows: first, randomization and rigid body energy minimization; second, semi-flexible simulated annealing; and third, flexible explicit solvent refinement. TSGA10 and BCL-2 residues involved in the binding were set to be 'active' residues, whereas neighbors of active residues were defined as 'passive' residues according to HADDOCK definition. Among the structures built by HADDOCK, the one with the lowest energy was selected for detailed analysis and display.

Statistical analysis

Data were presented as means ± SD and statistical analysis was performed by the t-test, one-way or two-way analysis of variance (ANOVA) followed by the Tukey test (Graph Pad Software, version 8.0, Inc, La Jolla, CA, USA). A P-value <0.05 was considered to be statistically significant. Each point or column represents the mean ± SD (n = 4–6). $P < 0.05$ (*), $P < 0.01$ (**), $P < 0.001$ (***) and $P < 0.0001$ (****).

Results

TSGA10 expression

After the stable transfection of HeLa cells and following clonal selection of transformed cells, overexpression of TSGA10 mRNA in HeLa-pcDNA3.1-TSGA10 (H.pc-TSGA10) and human fibroblast cells was shown as follows: Clone 1: 1.5 ± 0.34, clone 2: 3.4 ± 0.2, clone 3: 5.8 ± 0.38 and human fibroblast: 3.93 ± 0.45 folds increase in TSGA10 mRNA expression compared with HeLa-pcDNA 3.1 cells (H.pc) (3). Finally, we choose the clone 3 as densitometry analysis showed significantly increased TSGA10 protein expression compared with other ones (Fig. 1A). In clone 3, lowest cell viability was demonstrated following *TSGA10* overexpression. In addition, presence of TSGA10 protein and its overexpression were demonstrated by western blot (Fig. 1B) and immunocyhtochemistry analysis in transfected HeLa cells (Fig. 1C). Hypoxia significantly increased HIF-1α protein expression following TSGA10 overexpression (Fig. 1D).

TSGA10 overexpression induces autophagy

According to our findings, TSGA10 overexpression more than 5-folds caused an increased rate of autophagy in HeLa cells. We examined the HeLa-pcDNA3.1-TSGA10 (clone 3) due to its 5.8 folds increase in TSGA10 mRNA expression compared with HeLa-pcDNA 3.1 cells. Western blot analysis showed an increased not only in LC3II expression (Fig. 2A) but also in LC3II to LC3I proportion (autophagosome

formation index) in H.pc-TSGA10 cells compared with H.pc cells under normoxic and hypoxic conditions with and without 10mM ammonium chloride as an autolysosome inhibitor (Fig. 2B).

To investigate correlation between TSGA10 overexpression and autophagy we analyzed the expression level of autophagy-related genes such as Beclin1, BNIP3, NIX, ATG5, LC3I and LC3II in the H.pc-TSGA10 cells compared with H.pc cells in hypoxia and normoxia by real-time RT-PCR. Our findings indicated a significant increase in expression of autophagy-related genes in H.pc-TSGA10 cells compared with H.pc cells (Fig. 3. A-F). In order to measure the rate of autophagy, acridine orange staining was performed and the cells were analyzed using a fluorescence microscope. The percentage of cells with orange cytoplasm considering as autolysosome formation index was measured in for H.pc-TSGA10 cells compared with the H.pc cells under normoxic and hypoxic conditions with or without rapamycin (Rap) treatment. These findings showed the increased rate of acidic compartment in H.pc-TSGA10 cells compared with H.pc cells under various conditions (Fig. 3G).

TSGA10 overexpression induces apoptosis

To investigate apoptotic effects of *TSGA10* overexpression on HeLa cells, expression level of apoptosis-related genes BAX, BCL-2 and Caspase-3 were assessed by real-time RT-PCR. Real-time RT-PCR and Western blot analyses demonstrated a decreased expression of the BCL-2 and increased expression of BAX in H.pc-TSGA10 cells compared with H.pc cells in both normoxic and hypoxic conditions (Fig. 4A-C). Increased BAX/Bcl2 ratio as an apoptosis index was shown in H.pc-TSGA10 cells in comparison with control cells. This ratio demonstrated 2.4 ± 0.1 folds increase in normoxia and 4.3 ± 0.1 folds increase in hypoxia in compared to controls (Fig. 4D). Our findings clearly demonstrated an increased cleaved caspase-3 level in H.pc-TSGA10 cells compared with H.pc cells under normoxia and hypoxia. The procaspase-3 concentration in H.pc-TSGA10 cells was decreased in compared with controls and indicated increased cleavage of procaspase-3 to caspase-3 in stably transfected cells (Fig. 5). Increased level of caspase-3 in H.pc-TSGA10 cells confirmed the higher rate of apoptosis in these cells compared with controls.

TSGA10 **overexpression decreases cell viability**

The effect of the *TSGA10* overexpression on cell viability was evaluated by the MTT assay. Compared to the controls, cell viability was significantly decreased in *TSGA-10* overexpressing cells under both hypoxia and normoxia. It might be due to induced autophagy and apoptosis in these cells. In addition, cells treated with different concentrations of rapamycin as an autophagy inducer and cisplatin as an apoptosis inducer showed decreased cell viability in lower concentrations of these compounds in H.pc-TSGA10 cells compared with H.pc cells (Fig. 6A-D). MTT assay showed much less viability in HeLa cells transfected by pcDNA3.1-TSGA10 vector compared with HeLa cells transfected by pcDNA3.1 in various amount of used vector and rapamycin (Fig. 7A-D).

Molecular modeling and docking

The obtained alignment using six templates was introduced into MODELLER to generate 3D models of TSGA10. Ramachandran plot and summaries of structure models were obtained from PROCHECK program. Ramachandran plot analysis showed that main-chain conformations for 90.3% of amino acid residues are within the most favored or additionally allowed regions (Fig. 7A). In general, a score close to 100% implies a good stereochemical quality of the models (22). Therefore, the PROCHECK results suggested that the predicted models were of good quality.

Molecular docking by computer-assisted methods was used to improve our understanding of the interaction between TSGA10 and BCL-2 domains. The HADDOCK was used to calculate the possible conformation of the TSGA10 that binds to BCL-2 (Fig. 7B). To evaluate the binding capability of TSGA10, docking energy landscapes were analyzed. The values of total interaction energy, van der Waals energy and electrostatic energy are reported. Docking analysis revealed the significantly higher contribution of Coulombic forces, compared to Lenard-Jones interactions, in the binding of TSGA10 to BCL-2 (Table 1).

Table 1
Total interaction energy and its van der Waals and electrostatic components for the whole TSGA10/BCL-2 complex and important residue pairs involved

Interaction pair	VdW energy (kcal/mol)	Electrostatic energy (kcal/mol)	Interaction energy (kcal/mol)
TSGA10 – BCL-2	-43.0048	-253.236	-296.24
LYS169:HZ1 - ASP196:OD2	-0.86185	-29.5956	-30.4574
LYS169:HZ2 - GLU200:OE2	5.30767	-41.7245	-36.4168
ASP243:OD1 - ARG107:NH2	-1.01023	-17.9569	-18.9671
ARG512:HH11 - SER205:O	0.251528	-10.3206	-10.0691
ARG512:HH11 - MET206:O	-0.65217	-16.9378	-17.5899
GLU513:OE1 - ARG207:HH11	5.61914	-32.2724	-26.6533
LYS532:NZ - GLU200:OE1	-0.23984	-11.2684	-11.5083
ARG539:NH2 - ASP196:OD2	-0.81043	-21.3965	-22.2069
GLU691:OE1 - ARG207:NH2	0.663735	-36.8467	-36.1829

To gain a better understanding of the effects of each residue on binding affinity, a per-residue decomposition of the total energy was carried out to evaluate the energetic influences of critical residues on the binding in the TSGA10/BCL-2 complex. Intermolecular non-bonded interactions at the interface of the two proteins were detected in Discovery Studio, and residue pairs with lower binding energies were reported (Table 1). The van der Waals, electrostatic, and total interaction energies of these residues in the complex were determined with the 'Calculate Interaction Energy' protocol encoded in Discovery Studio. The complex was typed with CHARMM force field and the dielectric model was set to Implicit Distance-Dependent Dielectrics. All the other parameters were kept at their default values. As shown in Table 1, the contribution of the electrostatic component in the total interaction energy is greater than that of the hydrophobic interactions, for all reported residue pairs. Accordingly, all residue pairs indicate an interaction of side chains of charged amino acids from one interaction partner with side chains of polar/charged residues from the other. Therefore, van der Waals energies do not play a significant role in driving the formation of the TSGA10/BCL-2 complex. Compared with the other residue-residue interactions, LYS169-GLU200 and GLU691-ARG207 have the strongest electrostatic and total interaction energies.

Discussion

In the present study, H.pc-TSGA10 cells showed a higher expression of autophagy-related genes compared with H.pc cells under normoxic and hypoxic conditions. Acridine orange staining demonstrated higher acidic vesicles due to higher rate of autophagy in H.pc-TSGA10 cells in compared with H.pc cells under various conditions. Increased expression of BAX and BAX/Bcl2 ratio as an apoptosis index, increased cleaved caspase-3 level, and decreased expression of BCL-2 confirmed higher rate of apoptosis in H.pc-TSGA10 cells compared with H.pc cells in both normoxic and hypoxic conditions. Moreover, cell viability was significantly decreased in both stably and transiently transfected cells with pcDNA3.1-TSGA10 in the presence or absence of autophagy and apoptosis inducers under normoxic and hypoxic conditions.

Autophagy contributes in determining overall fate of the cells (23). Autophagy can used as a practical target in the clinic to destroy cancer cells by direct induction of type II programmed cell death (11). Defective function of Beclin 1, as a known regulator of autophagy and a tumor suppressor gene has been observed in several cancers. Increased expression of Beclin1 can induce autophagy and consequently prevent tumor development. The BCL-2/Adenovirus E1B 19kDa-intracting Protein 3-Like (BNIP3) and BNIP3 like (BNIP3L/NIX) genes, belonging to BCL-2 (BH3-Only) family, can induce autophagy-mediated cell death. BNIP3 and BNIP3L competes with Beclin1 in binding to BCL-2 or Bcl-xL and hence can lead to autophagy and mitophagy by separating Beclin1 from BCL-2 (24). Previous investigations have also illustrated that apoptosis inhibitors can induce autophagy by increasing level of Beclin1 and inhibiting formation of Beclin1/BCL-2 complex (25, 26). BNIP3L gene product plays important roles in the pathobiology of various diseases such as cancer. The modulated expression of BNIP3L during tumor hypoxia can directly influences tumor growth. Expression of this protein is required for an optimum

autophagy induction in hypoxic conditions needed its BH3 domains assists in competitively separating Beclin1 from Beclin/BCL-2 and Beclin/BCL-xL complexes (27–29).

Roghanian A, *et al.* have reported an inhibitory interaction between TSGA10 and vimentin (30). In addition, Wang RC, *et al*. have indicated that a drastic decrease in vimentin is associated with higher Beclin 1 levels which can consequently lead to increased autophagy (31). HIF-1α regulates autophagy by the induction of the expression of certain pro- and anti-apoptotic proteins such as BNIP3, BNIP3L and BCL-2 (32).

The ATG5 is an inducer of autophagy-dependent cell death, which can lead to LC3I to LC3II conversion. The LC3II contribute in autophagosome formation, thus, the expression level of this protein is associated with rate of autophagosome formation in mammalian cells (33). Our findings confirmed a significant increased expression of autophagy-related genes such as ATG5 and LC3II in H.pc-TSGA10 cells compared with H.pc cells, which indicated that overexpression of TSGA10, could significantly induce autophagy. ATG5, a simulator of autophagy-dependent cell death, plays a significant role in apoptosis as a downstream effector of caspases. Increased ATG5 activates apoptosis through calpain activation (33, 34).

In a previous study, we demonstrated that TSGA-10 overexpression caused decreased expression of angiogenic factors such as VEGF, CXCL12 and CXCR4 (3). Domigan, *et al*. showed that decreased levels of VEGF promoted mitochondrial fragmentation and lower glucose metabolism finally resulting in autophagy induction and cell death. Their findings showed that nhibiting VEGF expression led to increased autophagy by mean of rising FOXO activity (35). In addition, another study showed that increased bFGF levels decreased autophagy by inhibiting LC3 II (36). Hashmoto *et al*. reported that autophagy could be restricted by increased levels of progesterone which upregulates the expression of CXCL12/CXCR4 (37). Based on these findings, it seems that inhibiting angiogenesis via *TSGA10* overexpression induced autophagy in H.pc cells (Fig. 8)

According to a previous study, upregulation of TSGA10 induced autophagy through induction of P21. Induced P21 consequently inhibits BCL-2 (38). Therefore, *TSGA10* overexpression can indirectly promote autophagy and apoptosis by BCL-2 inhibition. Tumor cells overexpressing BCL-2 are quite resistant to apoptosis through downregulation of pro-apoptotic proteins, Bak and BAX. Considering important roles of BCL-2 in regulating apoptosis and autophagy, its inhibition would be promising in order to sensitize tumor cells to programmed cell death (PCD) (39, 40).

Furthermore, *TSGA10* overexpression can induce cell cycle arrest at G1/S through increasing levels of Rb, P53, P21, p16 which consequently leads to apoptosis (41). In our study, decreased cell viability following *TSGA10* overexpression was a consequence of activated apoptosis, which was mostly due to cell cycle arrest at G1/S and was partly due to BCL-2 inhibition. Based on a previous study, *TSGA10* overexpression decreased CXCL12, MMP2 and MMP9 expression by inhibiting HIF-1α (3). Decreased expression of MMP2 and MMP9 leads to CytC release and changes the expression levels of BAX and BCL-2 which consequently provokes apoptosis (42). In addition, decreased expression of CXCL12 and CCL25 has

shown lead to higher rate of apoptosis (43, 44). All the above-mentioned findings affirm that *TSGA10* overexpression can induce apoptosis via regulating multiple apoptotic targets (Fig. 8).

The TSGA10 gene, located on chromosome 2 (q11.2), consists of 19 exons and is associated with the sperm tail. Human TSGA10 is constituted of 698 amino acids. In mice, this protein is expressed in normal cells and tissues such as cerebellum, bone marrow, thyroid, brain, eye bulb, cecum, hematopoietic stem cells and testis. *TSGA10* overexpression has been detected in various conditions such as liver carcinoma, ovarian tumors, prostate, bladder, and colon cancer, malignant melanoma, cutaneous T-cell lymphoma and as well as autoimmune diseases. (1, 13, 45).

It has been widely accepted that TSGA10 plays a significant role in the spermatogenesis. In testis, falling oxygen level to less than 1% (hypoxic stress) compared with 2–9% in normoxic condition for many tissues of mammalian species is a disturbing agent for fetus development and is a risk factor for many pathologic conditions such as solid tumor, coronary artery ischemia and brain damages. Regarding high rates of cell proliferation and differentiation during spermatogenesis, being hypoxic causes dangerous condition and increased risk of tumor formation in testis tissue (15, 30, 46–48). Thus, expression level of HIF-1α and its downstream effectors regulating various cellular mechanisms is higher in testis in compared to other tissues. HIF-1α overexpression has been shown in various cancers. Cancer cells adapted to hypoxia are usually resistant to apoptosis and so, cancer treatment requires more aggressive strategies.

In testis cells with hypoxic microenvironment, it is crucial to identify the mechanisms regulating cell proliferation, cell cycle and survival in order to balance cell numbers and consequently, prevent testis cancer. TSGA10 can regulate this balance by inhibiting HIF-1α, which is expressed in higher levels in hypoxia compared with normoxia. Target genes of HIF-1α contribute in various cellular mechanisms such as apoptosis, angiogenesis, autophagy, glucose metabolism, erythropoiesis, tumor development and so on. In tumor development, HIF-1α plays an important role in establishing a balance between oxygen need and supply. HIF-1α is considered as a substantial molecule for adaptation of cells to stress like hypoxia by regulating expression of hundreds of genes. Inhibition of this molecule would hinder excessive cell proliferation and growth and thus could prevent cancer development. (3, 49, 50). Our previous investigation showed that a 55-kDa fragment of TSGA10 protein could inhibit HIF-1α:P300/CBP complex formation by binding to its TAD-C and PAS-B domain leading to HIF-1α inactivation. Therefore, this interaction indirectly resulted in BCL-2 inhibition (32).

Based on molecular docking results, eight out of the nine residues of BCL-2 which participate in its interaction with TSGA10 locate on its BH2 domain, which is shown to be required for the interaction with BAX and for anti-apoptotic activity (51). Thus, the possible molecular mechanism underlying the inhibition of BCL-2 by TSGA10 may be through covering its specific domain which mediates its oncogenic activity. Analysis of energies revealed a great negative free energy of TSGA10/BCL-2 interaction, where electrostatic attraction plays the major role in keeping the two proteins bound to each other. BCL-2 may attenuate inflammation by interaction with NLRP1, impairing NLRP1-inflammasome

activation (52). This binding is via the putative loop between motifs BH4 and BH3, which is not involved in the interaction with TSGA10.

Although the accurate function of TSGA10 gene is still not clearly understood, it seems that in addition to spermatogenesis, it is also contributed in autophagy and apoptosis. The present study is in agreement with those recognizing TSGA10 as a tumor suppressor gene (3). Our previous study illustrated that *TSGA10* overexpression could inhibit angiogenesis and tumor cell proliferation, migration and invasion by inhibiting HIF-1α (53). We demonstrated that in order to exerting antitumor effects of TSGA10 protein on cancer cells, its expression should reach a certain threshold. Thus, to apply TSGA10 as a tumor-suppressor, we used an expression vector with the highest rate of TSGA10 expression. In the present study, the role of TSGA10 in the induction of autophagy and apoptosis and decreasing cancer cell viability was shown. Since the TSGA10 is considerably expressed in various tumors, some studies have described it as a cancer testis antigen (CTA) (13, 15, 48). As a CTA, TSGA10 should be highly expressed only in testis, placenta and tumors, but it is widely expressed in normal human and mouse tissues. According to our present and previous studies, TSGA10 is not a CTA, but it is a tumor-associated marker with tumor suppressive function (3). This new function seems to be among cell regulatory mechanisms used to prevent tumor growth and development through autophagy and apoptosis inductions, thus, it might be considered as a promising candidate for cancer treatment and management.

Declarations

Author Contributions Statement

Study Design: Mohammad Hossein Modarresi, Davood Rezazadeh; Data Collection: Davood Rezazadeh, Kamran Mansouri, Ebrahim Barzegari; Statistical Analysis: Ebrahim Barzegari; Data Interpretation: Mohammad Hossein Modarresi; Fatemeh Ranjbarnejad; Manuscript Preparation: Davood Rezazadeh, Fatemeh Ranjbarnejad; Literature Search: Fatemeh Ranjbarnejad, Kamran Mansouri; Funds Collection: Mohammad Hossein Modarresi

Competing interests

The authors have no conflict of interests to declare.

Acknowledgements

We thank Dr. Mohammad Hossein Ghahramani, Dr. Elham Adham and Ms. Zohreh Hosseinkhani for providing critical reagents and excellent technical assistance. Funding for this project was provided by.

Funding

This work was supported by Department of Molecular Medicine, School of Advanced Technologies in Medicine, Tehran University of Medical Sciences [grant number 22021].

Data availability statements

Raw data were generated at Kermanshah University of Medical Sciences. Derived data supporting the findings of this study are available from the corresponding author on request.

References

1. Modarressi MH, Behnam B, Cheng M, Taylor KE, Wolfe J, van der Hoorn FA (2004). Tsga10 encodes a 65-kilodalton protein that is processed to the 27-kilodalton fibrous sheath protein. Biology of reproduction. 2004;70(3):608 – 15.
2. Hägele S, Behnam B, Borter E, Wolfe J, Paasch U, Lukashev D, et al. (2006). TSGA10 prevents nuclear localization of the hypoxia-inducible factor (HIF)-1α. FEBS letters. 2006;580(15):3731-8.
3. Mansouri K, Mostafie A, Rezazadeh D, Shahlaei M, Modarressi MH (2016). New function of TSGA10 gene in angiogenesis and tumor metastasis: a response to a challengeable paradox. Human molecular genetics. 2016;25(2):233 – 44.
4. Weidemann A, Johnson R (2008). Biology of HIF-1α. Cell Death & Differentiation. 2008;15(4):621-7.
5. Kaur J, Debnath J (2015). Autophagy at the crossroads of catabolism and anabolism. Nature Reviews Molecular Cell Biology. 2015;16(8):461 – 72.
6. Mancias JD, Kimmelman AC (2016). Mechanisms of selective autophagy in normal physiology and cancer. Journal of molecular biology. 2016;428(9):1659-80.
7. Mathew R, Karantza-Wadsworth V, White E (2007). Role of autophagy in cancer. Nature Reviews Cancer. 2007;7(12):961-7.
8. Kroemer G, Levine B (2008). Autophagic cell death: The story of a misnomer. Nature Reviews Molecular Cell Biology. 2008;9:1004-10.
9. Shen HM, Codogno P (2011). Autophagic cell death: Loch Ness monster or endangered species? Autophagy 2011;7:457 – 65.
10. Shen S, Kepp O, Kroemer G (2012). The end of autophagic cell death?. Autophagy. 2012;8:1–3.
11. Bialik S, Dasari SK, Kimchi A (2018). Autophagy-dependent cell death–where, how and why a cell eats itself to death. Journal of cell science. 2018;131(18):jcs215152.
12. Poon IK, Lucas CD, Rossi AG, Ravichandran KS (2014). Apoptotic cell clearance: basic biology and therapeutic potential. Nature Reviews Immunology. 2014;14(3):166 – 80.
13. Dianatpour M, Mehdipour P, Nayernia K, Mobasheri M-B, Ghafouri-Fard S, Savad S (2012). Expression of testis specific genes TSGA10, TEX101 and ODF3 in breast cancer. Iranian Red Crescent Medical Journal. 2012;14(11):719 – 23.
14. Capalbo D, Improda N, Esposito A, De Martino L, Barbieri F, Betterle C, et al. (2013). Autoimmune polyendocrinopathy-candidiasis-ectodermal dystrophy from the pediatric perspective. Journal of endocrinological investigation. 2013;36(10):903 – 12.

15. Mobasheri MB, Jahanzad I, Mohagheghi MA, Aarabi M, Farzan S, Modarressi MH (2007). Expression of two testis-specific genes, TSGA10 and SYCP3, in different cancers regarding to their pathological features. Cancer detection and prevention. 2007;31(4):296–302.
16. Yuan X, He J, Sun F, Gu J (2013). Effects and interactions of MiR-577 and TSGA10 in regulating esophageal squamous cell carcinoma. International journal of clinical and experimental pathology. 2013;6(12):2651.
17. Bian X, Yang Z, Feng H, Sun H, Liu Y (2017). A combination of species identification and STR profiling identifies cross-contaminated cells from 482 human tumor cell lines. Scientific reports. 2017;7(1):1–10.
18. Cavasotto CN, Phatak SS (2009). Homology modeling in drug discovery: current trends and applications. Drug discovery today. 2009;14(13–14):676 – 83.
19. Sali A, Blundell TL (1993). Comparative protein modelling by satisfaction of spatial restraints. Jounal of Molecular Biology. 1993;234:779–815.
20. Laskowski RA, MacArthur MW, Moss DS, Thornton JM (1993). PROCHECK: a program to check the stereochemical quality of protein structures. Journal of applied crystallography. 1993;26(2):283 – 91.
21. Dominguez C, Boelens R, Bonvin AM (2003). HADDOCK: a protein – protein docking approach based on biochemical or biophysical information. Journal of the American Chemical Society. 2003;125(7):1731-7.
22. Reddy CS, Vijayasarathy K, Srinivas E, Sastry GM, Sastry GN (2006). Homology modeling of membrane proteins: a critical assessment. Computational biology and chemistry. 2006;30(2):120-6.
23. Zaarour RF, Azakir B, Hajam EY, Nawafleh H, Zeinelabdin NA, Engelsen AS, et al. (2021). Role of hypoxia-mediated autophagy in tumor cell death and survival. Cancers. 2021;13(3):533.
24. Kang HP, Ihn H, Robertson DM, Chen X, Sugiyama O, Tang A, et al. (2021). Regional gene therapy for bone healing using a 3D printed scaffold in a rat femoral defect model. Journal of Biomedical Materials Research Part A. 2021;109(11):2346-56.
25. Won KY, Kim GY, Kim YW, Song JY, Lim S-J (2010). Clinicopathologic correlation of beclin-1 and bcl-2 expression in human breast cancer. Human pathology. 2010;41(1):107 – 12.
26. Pirtoli L, Cevenini G, Tini P, Vannini M, Oliveri G, Marsili S, et al. (2009). The prognostic role of Beclin 1 protein expression in high-grade gliomas. Autophagy. 2009;5(7):930-6.
27. Chien C-T, Shyue S-K, Lai M-K (2007). Bcl-xL augmentation potentially reduces ischemia/reperfusion induced proximal and distal tubular apoptosis and autophagy. Transplantation. 2007;84(9):1183-90.
28. Zhang J, Ney P (2008). NIX induces mitochondrial autophagy in reticulocytes. Autophagy. 2008;4(3):354-6.
29. Novak I, Kirkin V, McEwan DG, Zhang J, Wild P, Rozenknop A, et al. (2010). Nix is a selective autophagy receptor for mitochondrial clearance. EMBO reports. 2010;11(1):45–51.

30. Roghanian A, Jones DC, Pattisapu JV, Wolfe J, Young NT, Behnam B (2010). Filament-associated TSGA10 protein is expressed in professional antigen presenting cells and interacts with vimentin. Cellular immunology. 2010;265(2):120-6.
31. Wang RC, Wei Y, An Z, Zou Z, Xiao G, Bhagat G, et al. (2012). Akt-mediated regulation of autophagy and tumorigenesis through Beclin 1 phosphorylation. Science. 2012;338(6109):956-9.
32. Tracy K, Dibling BC, Spike BT, Knabb JR, Schumacker P, Macleod KF (2007). BNIP3 is an RB/E2F target gene required for hypoxia-induced autophagy. Molecular and cellular biology. 2007;27(17):6229-42.
33. Luo S, Rubinsztein D (2007). Atg5 and Bcl-2 provide novel insights into the interplay between apoptosis and autophagy. Cell death and differentiation. 2007;14(7):1247-9.
34. Shi M, Zhang T, Sun L, Luo Y, Liu D-H, Xie S-T, et al. (2013). Calpain, Atg5 and Bak play important roles in the crosstalk between apoptosis and autophagy induced by influx of extracellular calcium. Apoptosis. 2013;18(4):435 – 51.
35. Domigan CK, Warren CM, Antanesian V, Happel K, Ziyad S, Lee S, et al. (2015). Autocrine VEGF maintains endothelial survival through regulation of metabolism and autophagy. J Cell Sci. 2015;128(12):2236-48.
36. Zhang J, Liu J, Liu L, McKeehan WL, Wang F (2012). The fibroblast growth factor signaling axis controls cardiac stem cell differentiation through regulating autophagy. Autophagy. 2012;8(4):690-1.
37. Mei J, Zhu X-Y, Jin L-P, Duan Z-L, Li D-J, Li M-Q (2015). Estrogen promotes the survival of human secretory phase endometrial stromal cells via CXCL12/CXCR4 up-regulation-mediated autophagy inhibition. Human Reproduction. 2015:dev100.
38. Li X, Li X, Wang J, Ye Z, Li J-C (2012). Oridonin up-regulates expression of P21 and induces autophagy and apoptosis in human prostate cancer cells. Int J Biol Sci. 2012;8(6):901 – 12.
39. Rahmani M, Aust MM, Attkisson E, Williams DC, Ferreira-Gonzalez A, Grant S (2013). Dual inhibition of Bcl-2 and Bcl-xL strikingly enhances PI3K inhibition-induced apoptosis in human myeloid leukemia cells through a GSK3-and Bim-dependent mechanism. Cancer research. 2013;73(4):1340-51.
40. Liston P, Fong WG, Korneluk RG (2003). The inhibitors of apoptosis: there is more to life than Bcl2. Oncogene. 2003;22(53):8568-80.
41. Sakao S, Taraseviciene-Stewart L, Cool CD, Tada Y, Kasahara Y, Kurosu K, et al. (2007). VEGF-R blockade causes endothelial cell apoptosis, expansion of surviving CD34 + precursor cells and transdifferentiation to smooth muscle-like and neuronal-like cells. The FASEB Journal. 2007;21(13):3640-52.
42. Wang Z, Liu Z, Cao Z, Li L (2012). Allicin induces apoptosis in EL-4 cells in vitro by activation of expression of caspase-3 and-12 and up-regulation of the ratio of Bax/Bcl-2. Natural product research. 2012;26(11):1033-7.
43. Mao W, Yi X, Qin J, Tian M, Jin G (2014). CXCL12 inhibits cortical neuron apoptosis by increasing the ratio of Bcl-2/Bax after traumatic brain injury. International Journal of Neuroscience.

2014;124(4):281 – 90.
44. Kremer KN, Peterson KL, Schneider PA, Meng XW, Dai H, Hess AD, et al. (2013). CXCR4 chemokine receptor signaling induces apoptosis in acute myeloid leukemia cells via regulation of the Bcl-2 family members Bcl-XL, Noxa, and Bak. Journal of Biological Chemistry. 2013;288(32):22899-914.
45. Behnam B, Modarressi MH, Conti V, Taylor KE, Puliti A, Wolfe J (2006). Expression of Tsga10 sperm tail protein in embryogenesis and neural development: from cilium to cell division. Biochemical and biophysical research communications. 2006;344(4):1102-10.
46. Modarressi MH, Cameron J, Taylor KE, Wolfe J (2001). Identification and characterisation of a novel gene, TSGA10, expressed in testis. Gene. 2001;262(1):249 – 55.
47. Theinert S, Pronest M, Peris K, Sterry W, Walden P (2005). Identification of the testis-specific protein 10 (TSGA10) as serologically defined tumour-associated antigen in primary cutaneous T-cell lymphoma. British Journal of Dermatology. 2005;153(3):639 – 41.
48. Mobasheri MB, Modarressi MH, Shabani M, Asgarian H, Sharifian R-A, Vossough P, et al. (2006). Expression of the testis-specific gene, TSGA10, in Iranian patients with acute lymphoblastic leukemia (ALL). Leukemia research. 2006;30(7):883-9.
49. Maxwell PH, Wiesener MS, Chang G-W, Clifford SC, Vaux EC, Cockman ME, et al. (1999). The tumour suppressor protein VHL targets hypoxia-inducible factors for oxygen-dependent proteolysis. Nature. 1999;399(6733):271-5.
50. Salceda S, Caro J (1997). Hypoxia-inducible Factor 1α (HIF-1α) Protein Is Rapidly Degraded by the Ubiquitin-Proteasome System under Normoxic Conditions ITS STABILIZATION BY HYPOXIA DEPENDS ON REDOX-INDUCED CHANGES. Journal of Biological Chemistry. 1997;272(36):22642-7.
51. Yin X-M, Oltvai ZN, Korsmeyer SJ (1994). BH1 and BH2 domains of Bcl-2 are required for inhibition of apoptosis and heterodimerization with Bax. Nature. 1994;369(6478):321-3.
52. Bruey J-M, Bruey-Sedano N, Luciano F, Zhai D, Balpai R, Xu C, et al. (2007). Bcl-2 and Bcl-XL regulate proinflammatory caspase-1 activation by interaction with NALP1. Cell. 2007;129(1):45–56.
53. Amoorahim M, Valipour E, Hoseinkhani Z, Mahnam A, Rezazadeh D, Ansari M, et al. (2020). TSGA10 overexpression inhibits angiogenesis of HUVECs: A HIF-2α biased perspective. Microvascular research. 2020;128:103952.

Figures

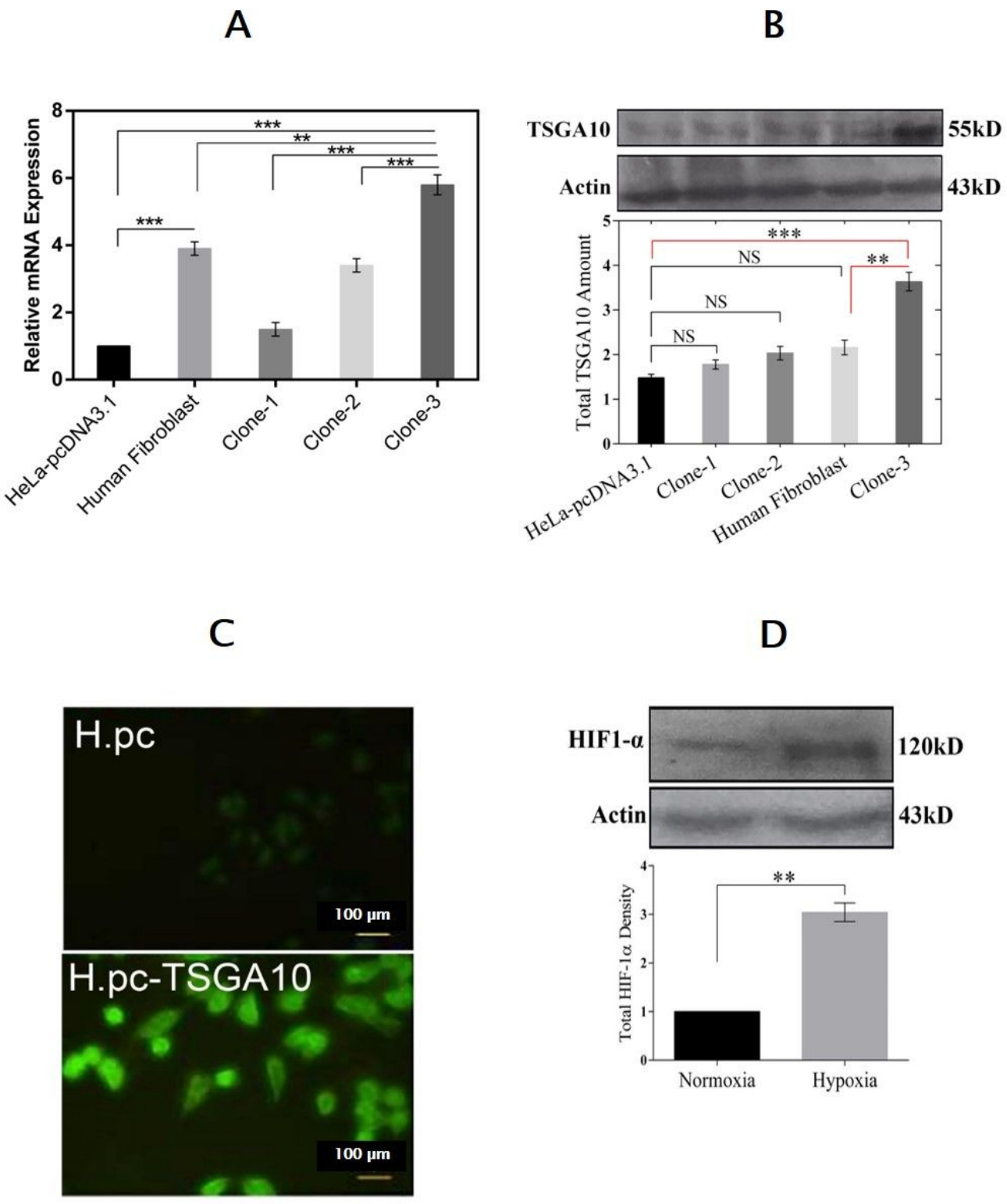

Figure 1

Relative expression of TSGA10 mRNA (A) and protein (B) (using western blot) in three clones of H.pc-TSGA10 compared with H.pc (as control) and human fibroblast cells (as normal cells). (C) Immunocytochemistry Analysis of TSGA10 in both H.pc and HeLa-pc-TSGA10 cells. (D) Effect of TSGA10 overexpression on HIF-1α level in H.pc-TSGA10 compared with control in both normoxic and hypoxic conditions by western blot analysis. HIF-1α protein expression was significantly higher in

hypoxia. Quantification of the protein bands in western blot analysis carried out using densitometric analysis (TotalLab software, Wales, UK). Protein amounts were normalized against beta-actin and compared with the control. Each data point was presented as mean ± SD from 5–6 independent experiments. **P < 0.01 and ***P < 0.001 compared with the control.

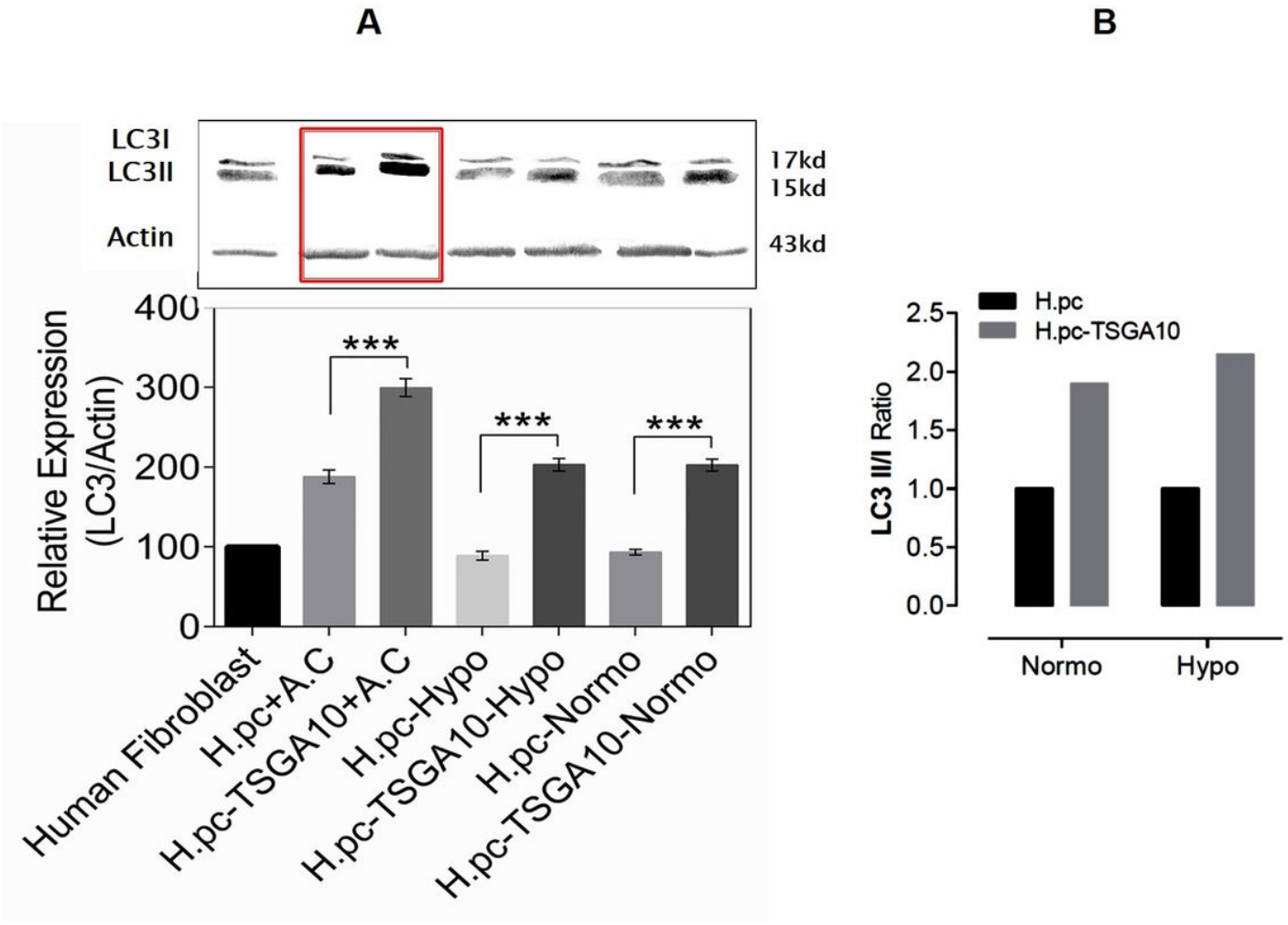

Figure 2

(A) Western blot analysis of Microtubule-Associated Protein 1 Light Chain 3 Alpha (LC3A) and Microtubule-Associated Protein 1 Light Chain 3 Beta (LC3B) in H.pc, H.pc-TSGA10 cells and human fibroblast incubated 24 h with or without 10 mM ammonium chloride (A.C) as autolysosome inhibitor in normoxia and hypoxia. (B) LC3 II/I ratio as the autophagosome formation index was significaltly increased in H.pc-TSGA10 cells. Each data point was presented as mean ± SD from 5-6 independent experiments. *P < 0.05, **P < 0.01 and ***P < 0.001 compared with the control.

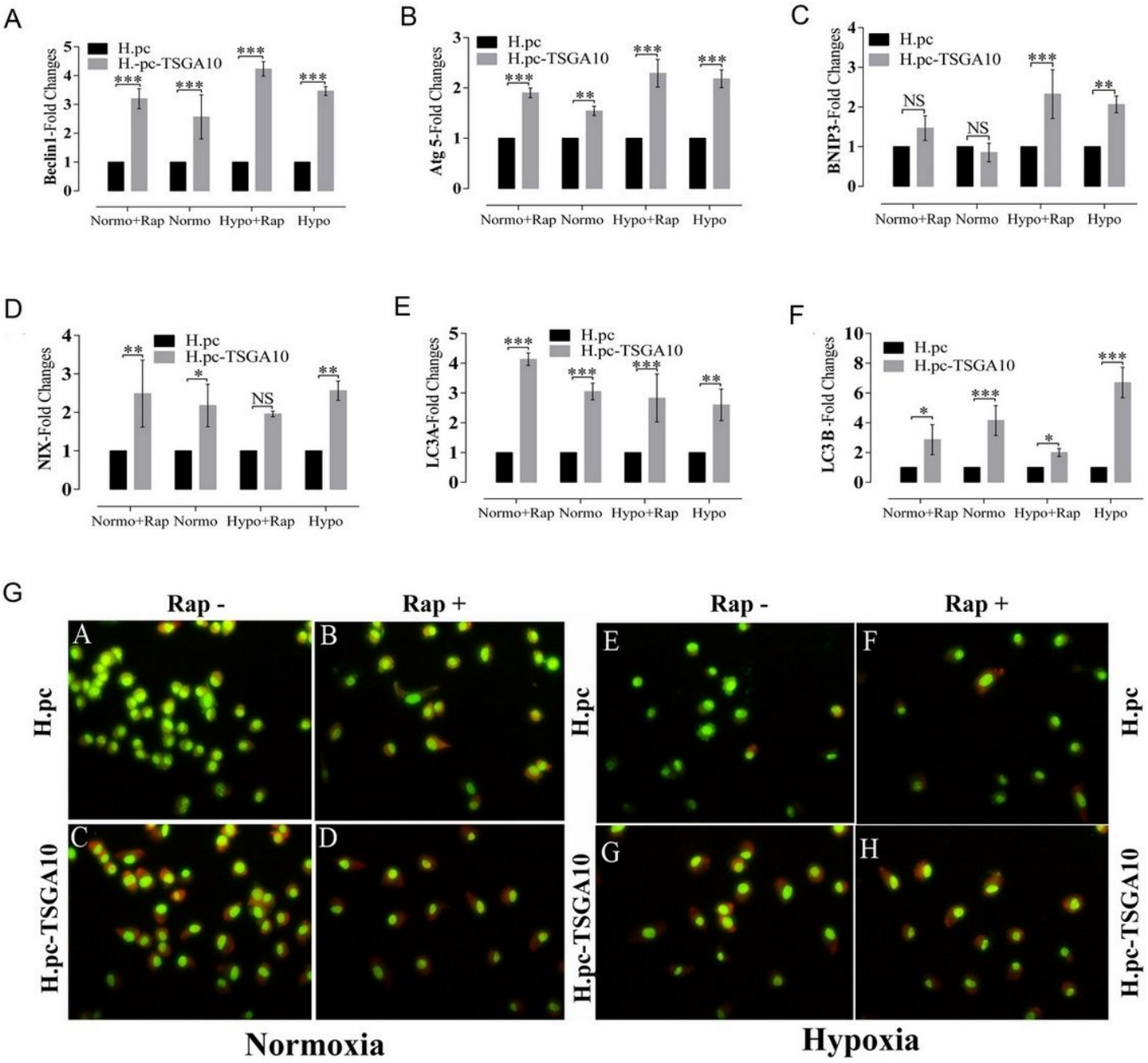

Figure 3

(A-F) Real-time RT-PCR analysis of autophagy-related genes such as Beclin 1, ATG-5, BNIP3, NIX, LC3A and LC3B respectively, in H.pc-TSGA10 cells compared with H.pc cells incubated under normoxia and hypoxia for 24 h with or without 100 nM Rapamycin treatment. (G) Acridine orange analysis in H.pc-TSGA10 cells compared with H.pc cells incubated under normoxia and hypoxia for 48 h with or without 100 nM Rapamycin treatment. Each data point was presented as mean ± SD from 5-6 independent experiments. *P < 0.05, **P < 0.01 and ***P < 0.001 compared with the control.

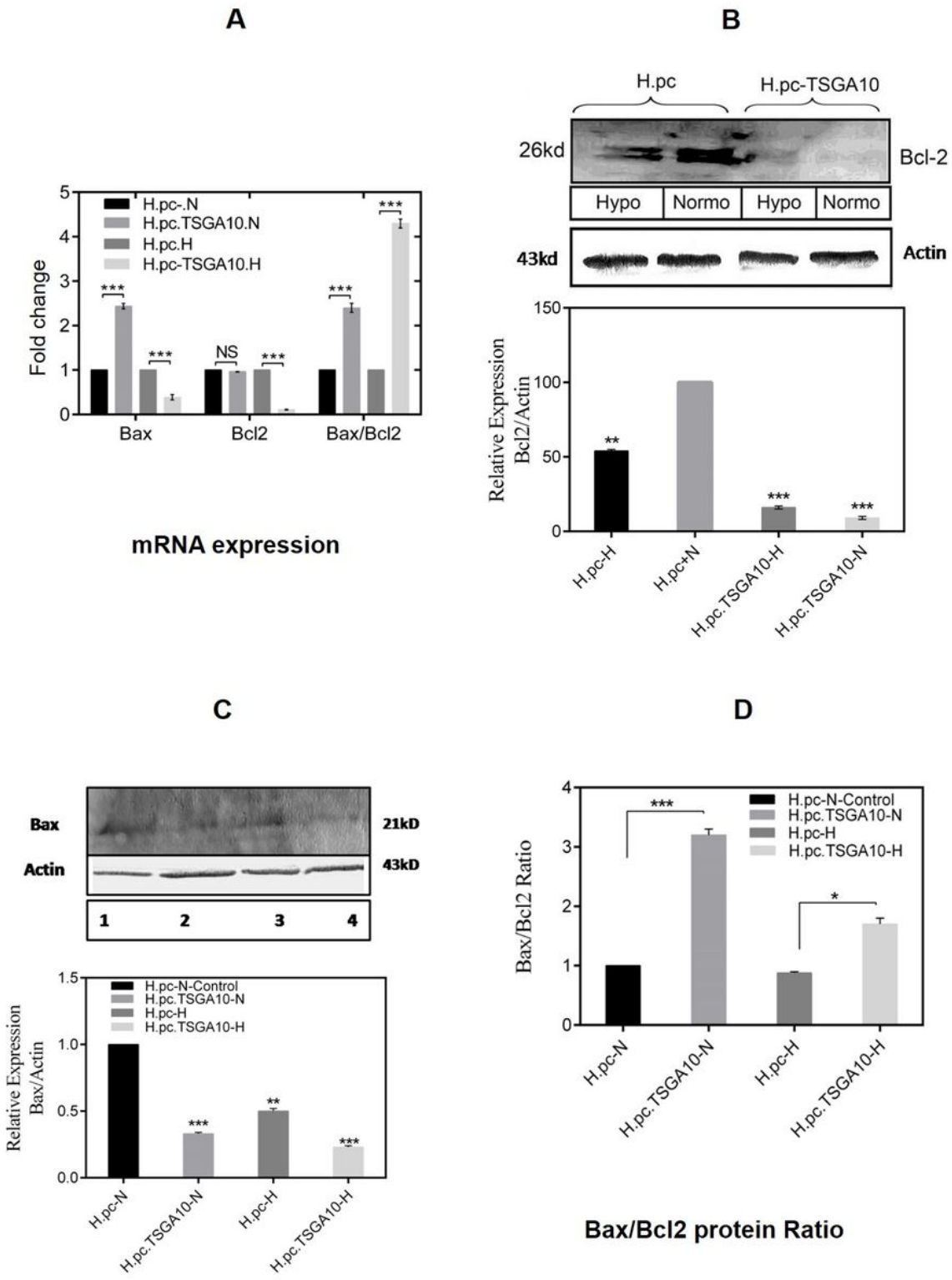

Figure 4

(A) Real-time RT-PCR analysis of apoptosis-related genes such as BAX and BCL-2 in H.pc-TSGA10 cells compared with H.pc cells incubated under normoxic (N) and hypoxic conditions (H) for 48 h. (B, C) Western analysis of BCL-2 and BAX expression, respectively. (D) BAX/BCL-2 protein ratios in H.pc-TSGA10 compared with H.pc cells incubated under normoxic (N) and hypoxic conditions (H) for 48 h

(n=4-5 independent experiments, mean ± SD. *P<0.05, **P < 0.01 and***P < 0.001 compared with the control).

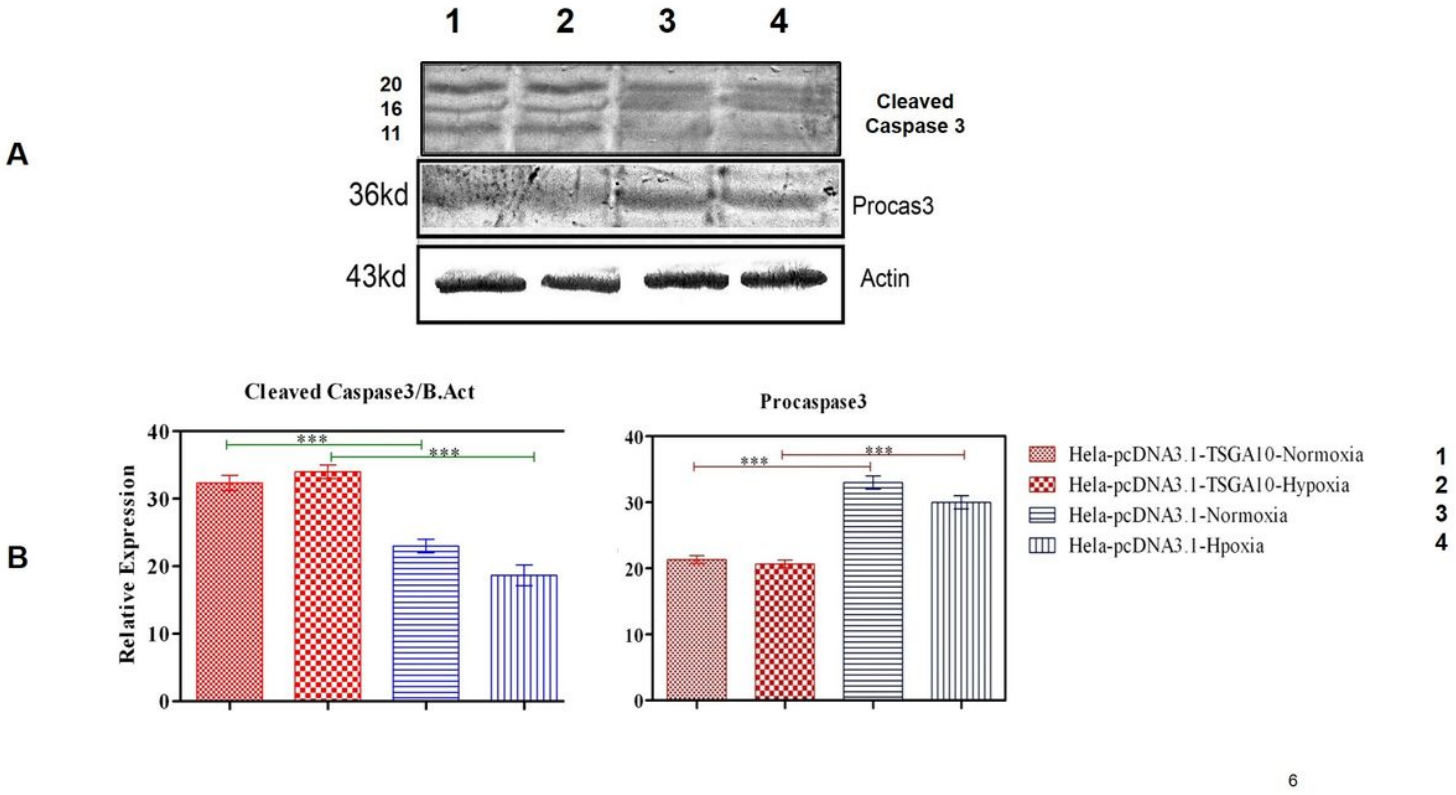

Figure 5

(A) Western analysis of procaspase-3 and cleaved caspase-3 expression. (B, C) Relative expression of procaspase-3 and cleaved caspase-3 in H.pc-TSGA10 cells compared with H.pc cells incubated under normoxic and hypoxic conditions for 48 h (n=4-5 independent experiments, mean ± SD. *P<0.05, **P < 0.01 and***P < 0.001 compared with the control).

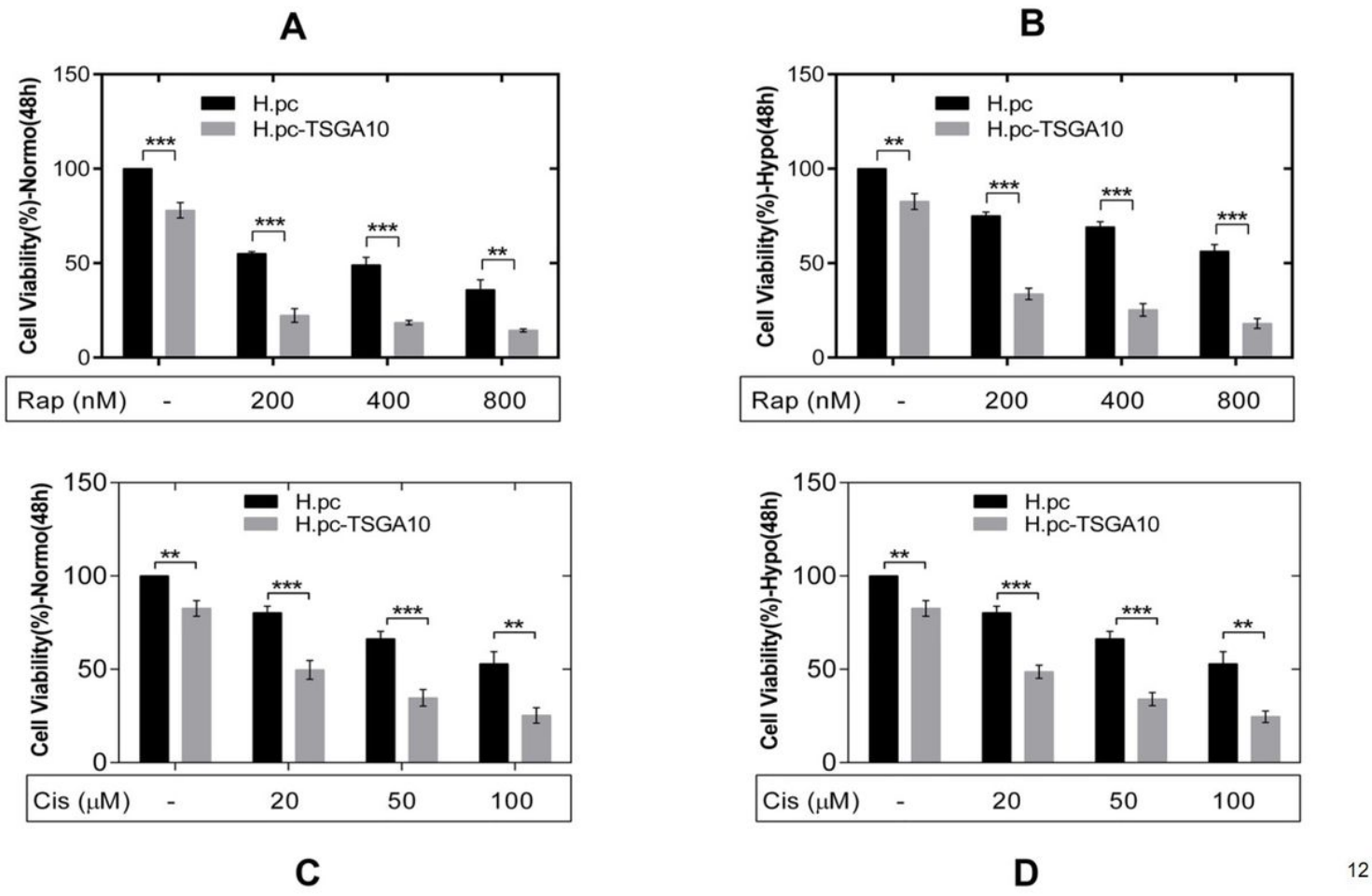

12

Figure 6

(A, B) Cell viability in H.pc-TSGA10 cells compared with H.pc cells treated with or without various concentrations of Rapamycin after 48 h incubation in normoxia and hypoxia, respectively. (C, D) Cell viability in H.pc-TSGA10 compared with H.pc treated with or without various concentrations of Cisplatin after 48 h incubation in normoxia and hypoxia, respectively (n = 6, mean ± SD, **P < 0.01, ***P < 0.001 compared with the control).

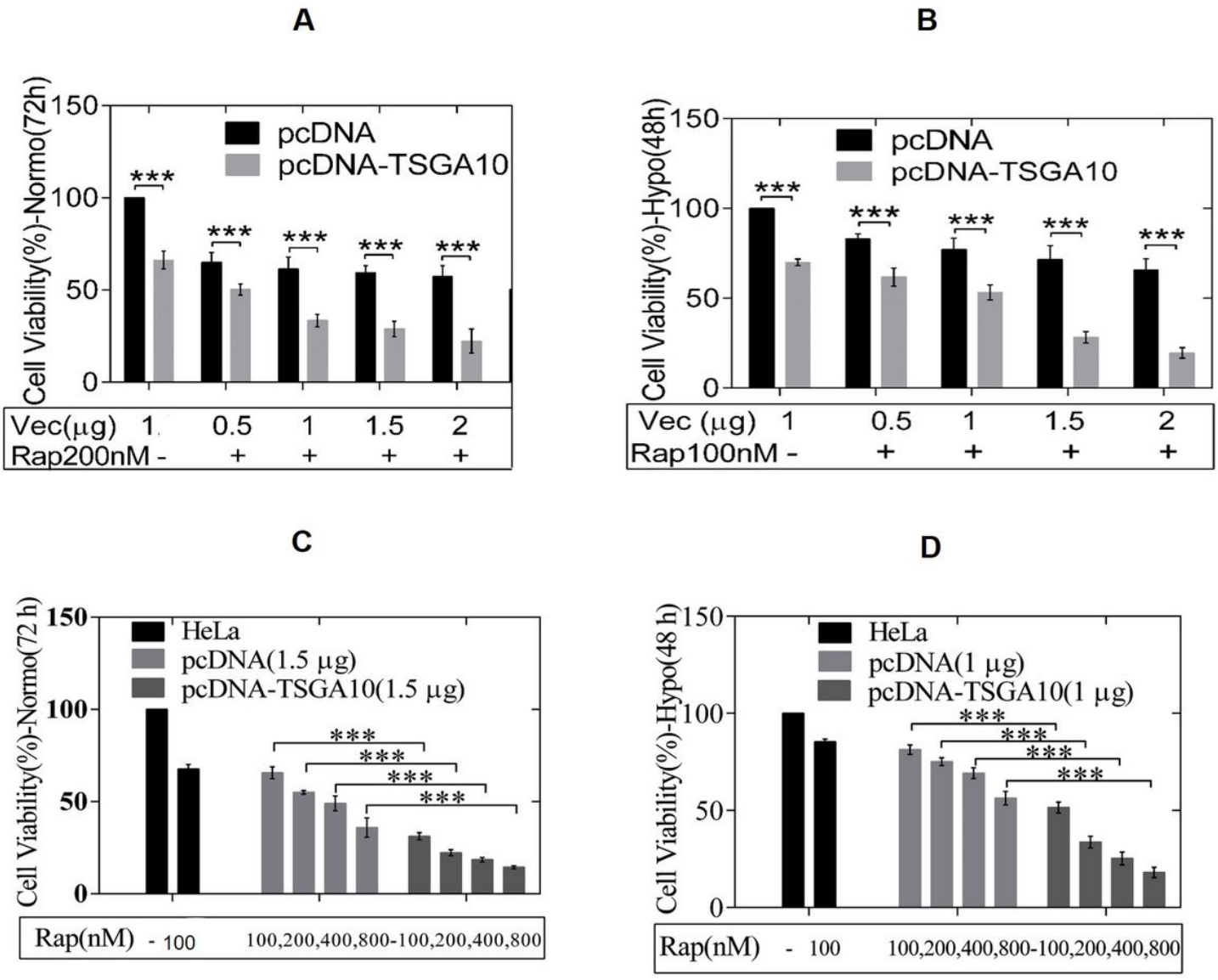

Figure 7

(A, B) HeLa cells were transfected with 1.5 μg pcDNA3.1-TSGA10 or pcDNA3.1 and then treated with or without various concentration of Rapamycin (100-800 nM) for 72 h in normoxia and hypoxia, respectively. (C, D) HeLa cells were transfected with various concentrations of pcDNA3.1-TSGA10 or pcDNA3.1 (0.5-2 μg) and then treated with or without 200 nM Rapamycin for 72 h in normoxia and hpoxia, respectively (n = 6, mean ± SD, **P < 0.01, ***P < 0.001 compared with the control).

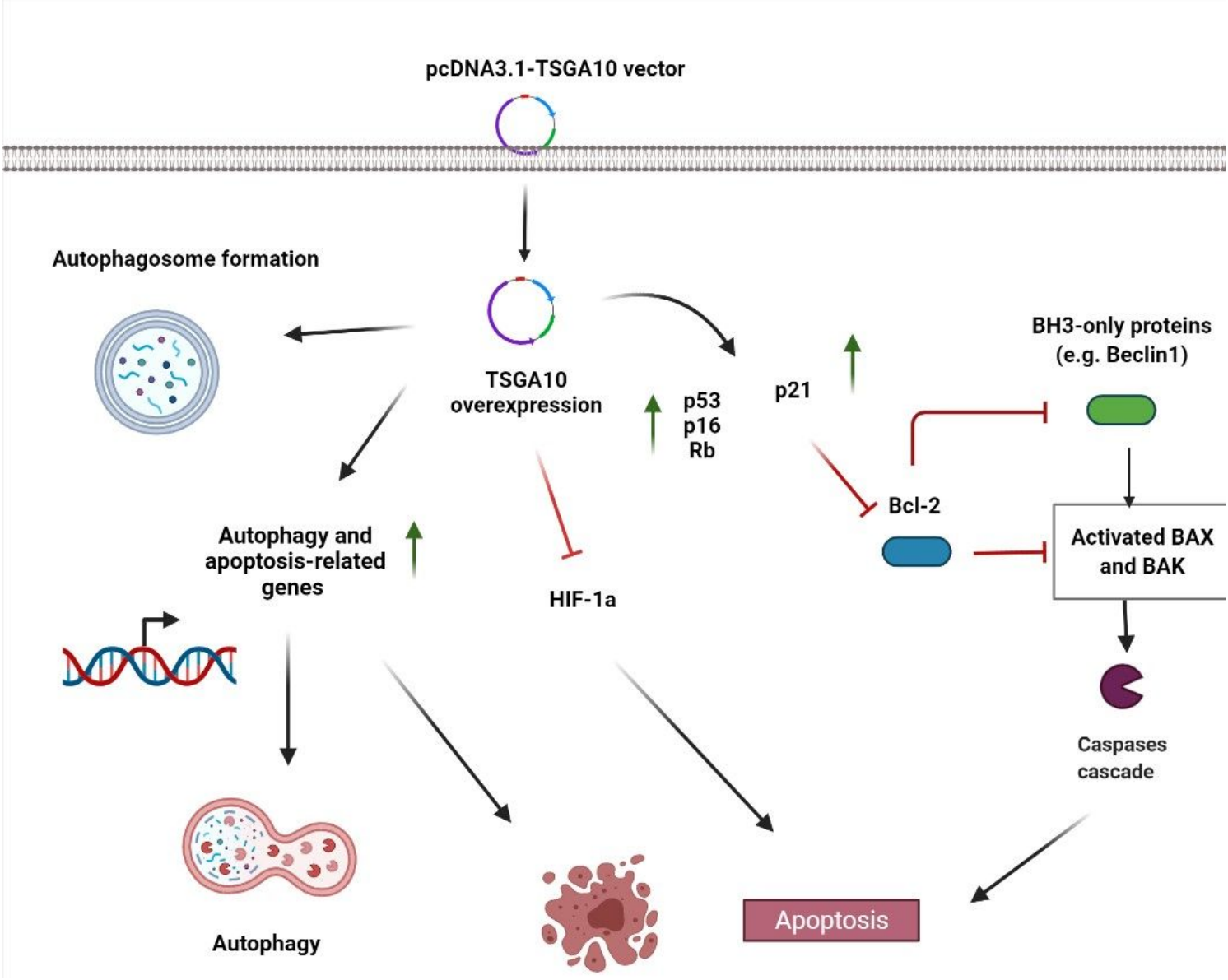

Figure 8

Schematic illustration of possible antitumor mechanisms of TSGA10 overexpression inducing autophagy and apoptosis mediated by inhibition of BCL-2 and HIF1-α.